Importance of Intrinsic Properties of Dense Caseinate Dispersions for Structure Formation

Julita M. Manski, Lieke E. van Riemsdijk, Atze J. van der Goot,* and Remko M. Boom

Food and Bioprocess Engineering Group, Wageningen University, P.O. Box 8129, 6700 EV Wageningen, The Netherlands

Received August 9, 2007

Rheological measurements of dense calcium caseinate and sodium caseinate dispersions (≥15%) provided insight into the factors determining shear-induced structure formation in caseinates. Calcium caseinate at a sufficiently high concentration (30%) was shown to form highly anisotropic structures during shearing and concurrent enzymatic cross-linking. In contrast, sodium caseinate formed isotropic structures using similar processing conditions. The main difference between the two types of caseinates is the counterion present, and as a consequence, the size of structural elements and their interactions. The rheological behavior of calcium caseinate and sodium caseinate reflected these differences, yielding non-monotonic and shear thinning flow behavior for calcium caseinate whereas sodium caseinate behaved only slightly shear thinning. It appears that the intrinsic properties of the dense caseinate dispersions, which are reflected in their rheological behavior, affect the structure formation that was found after applying shear. Therefore, rheological measurements are useful to obtain an indication of the structure formation potential of caseinate dispersions.

Introduction

Shear-induced structuring of proteins is of high interest for the development of novel products, such as meat analogues. Recently, we showed that well-defined flow and concurrent enzymatic cross-linking led to anisotropic materials based on dense calcium caseinate (Ca−caseinate) dispersions.[1] The study reported here demonstrates that the shear-induced structure formation as reported for Ca−caseinate is not generic yet. Dense sodium caseinate (Na−caseinate) dispersions formed isotropic materials using exactly the same processing conditions as for dense Ca−caseinate dispersions. Therefore, in this paper, we report on the difference between Ca−caseinate and Na−caseinate using rheological measurements to identify relevant prerequisites for the shear-induced formation of anisotropic structures in caseinate dispersions.

Shear-induced structure formation is widely investigated in polymer and micellar solutions and in colloidal suspensions using rheometers. The effects of shear flow can be summarized as the induction of three types of structures ranging from small distortions of the equilibrium structure, orientation in flow direction, and concentration fluctuations.[2,3] Viscoelasticity in terms of normal stresses as well as shear thinning behavior was thought to play an important role for shear-induced string formation of macroscopic particle dispersions.[4−7] Bundlelike ordering of dense colloidal latex dispersions was strongly affected by particle interactions and particle concentration.[8] Concentration fluctuations yielding shear bands have mainly been studied for wormlike micellar solutions.[9−12] Various studies showed that rheological measurements can be used as an indication whether shear-induced structure formation can occur. Those measurements reflect the presence of shear-induced concentration fluctuations or provide information on the physical properties of the structural elements in a dispersion.[3,10,13]

To our knowledge, research on concentrated caseinate systems is scarce. Several studies focused on the rheological behavior of concentrated Na−caseinate,[14] casein,[15,16] and milk[17−19] to couple shear viscosity with physical properties of the protein micelles, such as voluminosity and interaction potentials. Concentrated Na−caseinate dispersions above 10% (w/v) were found to behave as closely packed spheres exhibiting soft sphere interactions.[14] Similarly, jamming of β-casein above 10% (w/v) was reported to cause a strong increase in viscosity, reflecting the closely packed character of the dispersions.[16] The micelles present in caseinate dispersions range from 20 to 50 nm for Na−caseinate[20] and from 100 to 300 nm for Ca−caseinate in diameter.[21,22] The difference in micelle size is attributed to the presence of calcium ions that provide interaction with casein proteins leading to larger micelle sizes.[23]

Many studies, concerned with structure evolution under shear, relate the macroscale phenomena (structuring) to rheological behavior by using well-defined flow for structure formation, which allows such a comparison. In line with this, the objective of the study reported here was to investigate whether the structure formation of the caseinates at the macroscale using well-defined flow could be related to the rheological properties of the concentrated starting materials. The structure formation of both caseinates (30%) in the presence of a dispersed phase (fat) was investigated in a shear cell device providing well-defined flow fields, followed by structure analysis using mechanical tests and microscopy (scanning electron microscopy (SEM) and confocal scanning laser microscopy (CSLM)). The rheological behavior of both caseinates (15−30%) was characterized using steady shear, step−strain, and small-amplitude oscillatory shear measurements.

Experimental Section

Materials. Both Ca−caseinate and Na−caseinate contained at least 88% protein according to the manufacturer's specifications (DMV International, Veghel, The Netherlands). Ca−caseinate contained 1.47%

* Author to whom correspondence should be addressed. Phone: +31 317 484372. Fax: +31 317 482237. E-mail: atzejan.vandergoot@wur.nl.

10.1021/bm700885f CCC: $37.00
Published on Web 10/12/2007

calcium and 0.01% sodium, whereas Na−caseinate contained 1.49% sodium, which was determined using an inductively coupled plasma mass spectrometer. Depending on the concentration used, protein dispersions (pH 6.8−7.0) were either prepared by mechanical stirring overnight (protein concentration ≤20% w/w) or by preparing a so-called premix (protein concentration >20% w/w). The premix of caseinate and demineralized water was prepared in a kitchen mixer at low speed and room temperature prior to processing. Several minor components were added for preservation and CSLM analysis, being 1% (w/w) sodium benzoate (Sigma-Aldrich, Zwijndrecht, The Netherlands) and 2×10^{-4}% (w/w) rhodamine 110 (catalogue no. 83695, Sigma-Aldrich), respectively. The latter was added to the protein premix as a 0.02 g L^{-1} solution in phosphate-buffered saline (PBS).

In the case of an enzyme treatment, microbial Ca^{2+}-independent transglutaminase (Tgase; protein−glutamine:amine γ-glutamyl-transferase, EC 2.3.2.13) derived from *Streptoverticilium moberansae* (1% Tgase, 99% maltodextrine, Ajinomoto Co. Inc., Tokyo, Japan) was added to the aqueous part of the premix (expressed as enzyme−protein ratios E:P = 1:20). For this purpose, a 20% (w/w in demineralized water) Tgase stock solution was prepared freshly prior to the experimental runs by mechanical stirring at room temperature for 1 h. The measured activity of Tgase was 117 units g^{-1} using the hydroxamate method.[24]

Palm fat, acquired from Barentz Raw Materials (Hoofddorp, The Netherlands), was used as a dispersed phase in selected protein materials. Nile Red (catalogue no. 72485, Sigma-Aldrich), a fluorescent dye for fat for CSLM, was added to the melted palm fat in a concentration of 0.2 g L^{-1}. Of this undiluted solution, 15% v/v was shortly mixed by hand with an appropriate amount of the protein premix prior to transferring the protein−fat mixture to the shear cell device.

Dimethylsulfoxide (DMSO) and ethanol, used for preparation of samples for SEM, were of analytical grade (Sigma-Aldrich).

Preparation and Analysis of Caseinate Materials. Dense Na−caseinate dispersions (30%) were sheared in the shear cell device in the absence or presence of the cross-linking enzyme transglutaminase (E:P = 1:20), similarly to the methods that were used for preparing dense Ca−caseinate materials. After preparing the Na−caseinate materials in the shear cell device, tensile tests were performed to determine the yield stress and yield strain measured parallel and perpendicular to the shear flow. The samples were analyzed using CSLM and SEM as described elsewhere.[25]

Rheological Characterization of Dense Caseinate Dispersions. *Steady Shear Measurements.* Shear rate sweeps including the measurement of normal forces were performed for Ca− and Na−caseinate at various concentrations (15%, 20%, 25%, and 30% Ca−caseinate and 15%, 20%, and 30% Na−caseinate) with a Paar MCR 301 rheometer (Anton Paar, Graz, Austria) at 50 °C using cone/plate geometries (i.e., angle 4°/diameter 50 mm for 15% and 20% protein and angle 2°/diameter 20 mm for 25% and 30% protein due to the large viscosity spectrum). All dispersions contained 1% sodium benzoate. The 15% and 20% protein dispersions were liquid when loaded to the rheometer, whereas 25% and 30% protein dispersions were soft solids, which became liquid upon heating. Shortly before the rheological characterization, the soft solids were prepared in a Brabender Do-Corder mixer (type W50) at 50 °C and 50 rpm for 20 min (of which the first 5 min were mixed at 5 rpm) to obtain well-dispersed starting materials. The 15% and 20% protein dispersions were dispersed overnight prior to the rheological measurements and kept at ∼40 °C. Water evaporation during the measurements was minimized by using a solvent trap. After temperature equilibration (2 min), duplicate (except for 30% caseinates) shear rate sweeps were performed in the range of 1−300 s^{-1}. Each shear rate was applied for 10 s (total measure time 210 s). After applying increasing shear rates (up sweep), the shear rate was decreased to measure the down sweep. For 30% Ca−caseinate and 30% Na−caseinate, the effect of preshear (5 and 25 s^{-1} for 2 min) was investigated, and the effect of a resting time (7 min followed by preshear) before applying a new shear rate sweep on the same sample.

The transient viscosity behavior of the same protein dispersions (except for 25% Ca−caseinate) was measured at constant shear rates (24, 50, and 120 s^{-1}) for >1000 s. Prior to the transient measurements at these constant shear rates, the shear rate was increased stepwise: 1, 10 (followed by 24 or 50 s^{-1}), and 100 s^{-1} (followed by 120 s^{-1}), each applied for 100 s. The shear stress and first normal stress difference (N_1) determined after 60 s of shearing at these shear rates (average values of at least duplicates) were compared to the measured values obtained during the shear rate sweeps.

To ensure that the measured flow curves were not affected by edge instabilities and other artifacts, flow curves of 30% Ca−caseinate were measured using various gap sizes (2−10 times the normal gap size for a cone and plate of angle 2°/diameter 20 mm). A flow curve was also measured using a larger cone and plate (angle 4°/diameter 50 mm). These curves (not shown) resemble the presented flow curves in Figure 4.

The difficulty of measuring dense protein systems is reflected in the maximum values of the coefficient of variation (CV, defined as the ratio of standard deviation and mean value multiplied by 100%) for the measured stress values. The maximum CV for shear rate sweeps as well as transient measurements was 9% for 15% and 20% Na−caseinate; 30% Na−caseinate showed a maximum CV of 30% for transient stress values. The CV values for the shear rate sweeps of 15% Ca−caseinate were <125% for shear rates below 10 s^{-1}, and a maximum CV of 13% for shear rates exceeding 10 s^{-1}. The maximum CV for 20% Ca−caseinate was 39%. The maximum CV for the measured transient stress values were 32%, 28%, and 54% for 15%, 20%, and 30% Ca−caseinate, respectively.

Step−Strain Measurements. Step−strain measurements were performed at 50 °C using a stress-controlled Paar MCR 301. A small cone/plate geometry (angle 2°/diameter 20 mm) was applied for 25% and 30% Ca−caseinate and 30% Na−caseinate whereas a large cone/plate geometry (angle 4°/diameter 50 mm) was used for 20% Ca−caseinate. Five strain levels from the nonlinear region were applied for ∼16 min, i.e., 10%, 50%, 100%, 200%, and 400% strain. The relaxation modulus as function of time measured at the various train levels was compared for the four caseinate dispersions measured. The step−strain measurements were performed once.

Small-Amplitude Oscillatory Shear Measurements. Frequency sweeps (angular frequency ω range of 1−628 s^{-1}) were performed at a constant strain of 1% (based on strain amplitude sweeps performed at 1 Hz) at 50 °C using a stress-controlled Paar MCR 301. The serrated parallel-plate geometry (diameter 25 mm, gap 1 mm) was used for 25% (single measurement) and 30% (duplicate) Ca−caseinate and 30% Na−caseinate (duplicate), because parallel plates are the preferred geometry for small strain measurements of highly viscous materials.[26] A cone/plate (angle 4°/diameter 50 mm) was used for 20% Ca−caseinate (single measurement). The CV in the G' measurements for Na−caseinate was below 10% for ω < 300 s^{-1}, and the maximum CV was 23%. The maximum CV for Ca−caseinate was 45%.

Results and Discussion

This section will show the difference in structure formation of Na−caseinate and Ca−caseinate and in their rheological properties.

Effect of Shear on Structure Formation of Dense Ca− and Na−Caseinate Dispersions. As shown previously, 30% Ca−caseinate dispersions form highly anisotropic materials under shear flow.[1,25] Figure 1 illustrates the anisotropic, fibrous structure that was formed after shearing and cross-linking of 30% Ca−caseinate. Besides fibrous structures, also layered structures were encountered after shearing 30% Ca−caseinate in the absence of the cross-linking enzyme Tgase. In the current paper, we show that dense 30% Na−caseinate dispersions remained isotropic after identical processing (shearing at 120

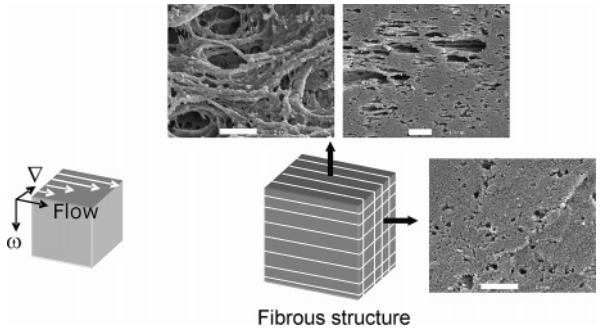

Figure 1. Schematic representation of the fibrous structure formed after shearing 30% Ca−caseinate in the presence of the cross-linking enzyme transglutaminase. SEM images obtained at two fracture planes display the microstructures of the sheared Ca−caseinate dispersion, which are described in detail elsewhere.[1] The scale bars denote 1 μm.

Table 1. Ratio of Tensile Properties Measured Parallel and Perpendicular to the Shear Flow of Sheared and Cross-Linked Na−Caseinate Materials with or without Palm Fat[a]

material	yield stress $\sigma_{\parallel}/\sigma_{\perp}$	yield strain $\epsilon_{\parallel}/\epsilon_{\perp}$
30% Na + Fat	0.8 ± 46%	0.9 ± 16%
30% Na	1.1 ± 85%	1.0 ± 42%
30% Ca + Fat [25]	8.2 ± 38%	2.6 ± 18%
30% Ca [1]	9.2 ± 24%	2.6 ± 8%

[a] The ratio values for Ca−caseinate are included for comparison. All of the materials comprised 30% protein and Tgase (E:P = 1:20) and were prepared by shearing at 120 s^{-1} for 30 min. Materials with palm fat contained 15% (v/v) palm fat. The yield stress and yield strain ratio values include 95% confidence intervals.

s^{-1} and cross-linking with Tgase 1:20 for 30 min). A homogeneous macrostructure was observed, both in the absence and in the presence of fat. Tensile tests of sheared and cross-linked Na−caseinate (with or without palm fat) confirmed that the material behaved as an isotropic material when comparing the yield stress and yield strain values parallel and perpendicular to the exerted shear flow in the shear cell device, which resulted in ratio values around one as shown in Table 1. The mesostructure of sheared and cross-linked Na−caseinate−fat material showed that fat was present as droplets, randomly located in the matrix, as displayed in Figure 2. SEM images of the microstructure parallel (Figure 3A) and perpendicular (Figure 3B) to the shear flow showed that no molecular or mesoscale alignment was achieved in the sheared and cross-linked Na−caseinate−fat material.

Table 2 summarizes the various observations with respect to dense caseinate systems and the effect of shear and cross-linking on the resulting structures. These experiments indicate that the alignment was specific for the protein Ca−caseinate and was influenced by protein concentration, because shearing and cross-linking of 20% Ca−caseinate yielded an isotropic material. The presence of a dispersed phase did not alter the structure formation of the protein phase.

The difference found in structure formation of 30% Ca−caseinate and 30% Na−caseinate leads to the hypothesis that the cause for this difference lays in the fundamental differences of the physical properties of the starting materials. Shear can only induce structure in these systems if its effect cannot be compensated by the mobility of the system. Therefore, we think that the intrinsic physical properties of 30% Ca−caseinate are such that shear-induced structure formation is favored at the time scales that we investigated, in contrast to Na−caseinate. We observed an effect of Ca−caseinate concentration as shearing and cross-linking of 20% Ca−caseinate yielded isotropic structures, which is in contrast with the anisotropic structures obtained for 25% and 30% Ca−caseinate. The fact that the Ca−caseinate concentration affects the structure being formed suggests that not only the physical properties of the structural elements play a role but also the density of those elements. In addition, the structure formation in terms of orientation that we found for the dense Ca−caseinate dispersions seems analogous to the structure formation in polymer (micellar) solutions and colloidal suspensions that is attributed to so-called shear banding or flow-induced formation of concentration fluctuations.[27−29] To shed light on the drivers for structure formation of the caseinate dispersions, we performed rheological measurements.

Rheology of Dense Ca− and Na−Caseinate Dispersions. *Effect of Steady Shear on Shear Stress.* Figure 4 depicts the shear stress as function of shear rate of Ca− and Na−caseinate at various concentrations (i.e., 15%, 20%, 25%, and 30% for Ca−caseinate and 15%, 20%, and 30% for Na−caseinate) in the range of 1−300 s^{-1}. The main difference between the shear stresses of Ca− and Na−caseinate is that the shear stress is much smoother for Na−caseinate at all concentrations. Further, Ca−caseinate shows complex behavior whereas Na−caseinate behaves slightly shear thinning at the concentrations and shear rates measured. At a low shear rate, the 30% caseinate dispersions show an anomalous behavior, which may be attributed to the presence of an (apparent) yield stress or start-up effect caused by their solidlike character.

At all four concentrations, Ca−caseinate exhibits fluctuations in shear stress with increasing shear rate. First, an instability is observed, and when the shear rate exceeds approximately 10 s^{-1}, the curves for all Ca−caseinate concentrations become monotonic; they all show shear thinning behavior. An increase in stress may reflect the buildup of structure, whereas the stress decrease indicates breakup of this structure. The non-monotonic evolution of the stress is often explained by transition(s) in "structure" in the case of micellar dispersions.[30] For micellar suspensions, an instability in the flow curve is sometimes referred to as "spurt" or "top-jumping".[10,13] However, it may be doubtful whether the observed instability in the 30% Ca−caseinate dispersion can be interpreted along those lines of reasoning.

On the basis of preliminary shear rate sweeps that were performed using various measure times as well as transient measurements at fixed shear rates, we can conclude that the shear stresses of both caseinates depended on the shear time applied. A too short shear time, i.e., less than 5 s, led to deviating flow curves, suggesting that no steady state was reached (data not shown). A good resemblance was found between transient flow data obtained at a constant shear rate (data taken at $t = 60$ s) and shear rate sweeps where a constant shear rate sweep of 10 s per shear rate was applied, which is shown in Figure 4. It must be noted that the transient shear stress showed an overshoot during the start-up flow for dense Ca−caseinate (20% or 30%) dispersions, whereas no such overshoot was observed for Na−caseinate. This suggests again that some form of structure was present in the dense Ca−caseinate dispersions.

The occurrence of the instability in the flow curve of 30% Ca−caseinate, and to lesser extent for 25% Ca−caseinate, shows similarities with the shear thickening behavior prior to shear thinning that was observed for dense β-casein suspensions. Panouillé et al.[16] related this behavior to the presence of an attractive force between the closely packed micelles. In Ca−caseinate dispersions, calcium ions provide strong interactions between proteins.[23] These interactions can lead to gradual protein

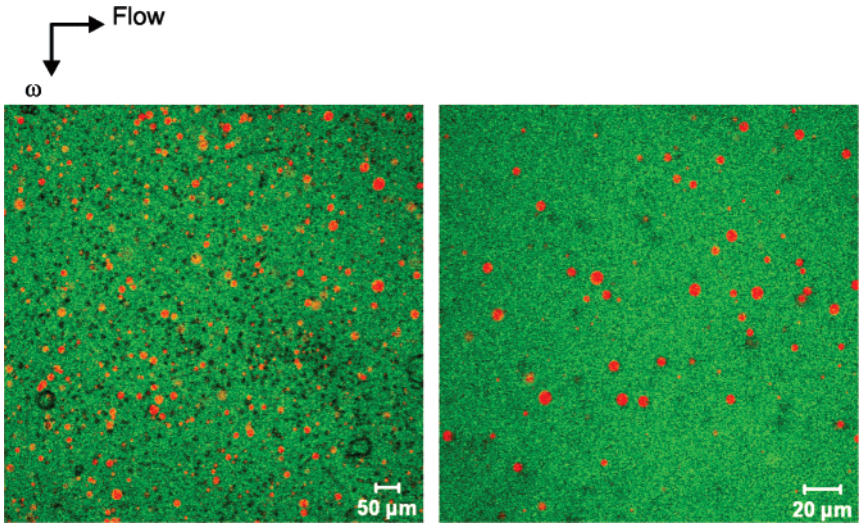

Figure 2. CSLM images of sheared and cross-linked 30% Na−caseinate and 15% fat (Tgase 1:20, 120 s^{-1}, 30 min, 50 °C) obtained at two magnifications (10×, scale bar 50 μm, and 40×, scale bar 20 μm).

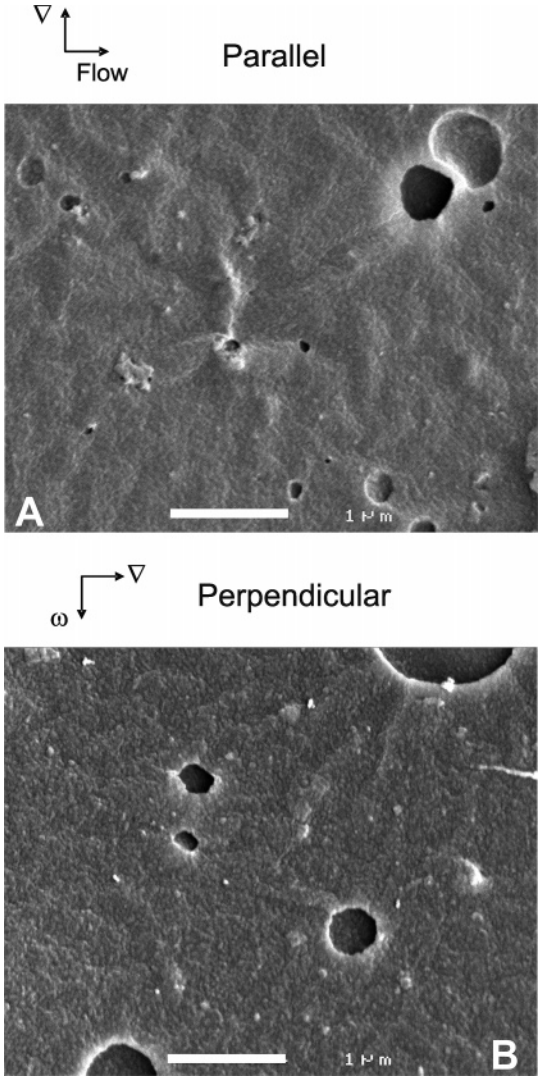

Figure 3. SEM images of sheared and cross-linked 30% Na−caseinate and fat (Tgase 1:20, 120 s^{-1}, 30 min) parallel (A) and perpendicular (B) to the shear flow exerted in the shear cell device. The scale bars denote 1 μm.

aggregation and calcium-bridge formation. The absence of a zero-shear viscosity plateau indicates that large aggregates are present in Ca−caseinate dispersions.[31] A similar observation

Table 2. Overview of Observations of the Structural Properties of Ca−Caseinate and Na−Caseinate Materials after Shearing (120 s^{-1}) and Cross-Linking Using Tgase for 30 min (unless Stated Otherwise)

protein	concentration (%)	E:P	dispersed phase	structural properties
Ca−caseinate	30	1:20	15% fat	anisotropic (fibers)[25]
		1:20		anisotropic (fibers)[1] anisotropic (layers)[1]
	25	1:17	15% fat	anisotropic[25]
	20	1:10		isotropic (syneresis)[a]
		1:20	10% fat	isotropic
Na−caseinate	30	1:10	10% Fat	isotropic
		1:20	15% fat	isotropic
		1:20		isotropic[b]
	20	1:20	10% fat	isotropic[c]

[a] 60 min of shearing. [b] Isotropic after applying 120 and 360 s^{-1}. [c] 40 min of shearing.

was done for closely packed latex suspensions.[2] Instabilities were also observed in the flow curves of the less dense Ca−caseinate dispersions, i.e., 15% and 20%, but these occurred at lower shear stress values. This suggests that these dispersions were more liquidlike compared to 25% and 30% Ca−caseinate due to the presence of a lower number of aggregates.

Various preshear treatments (5 and 25 s^{-1} for 2 min) did not result in the breakdown of the structure present in 30% Ca−caseinate, as we still observed an initial increase in shear stress, which may be apparent shear thickening behavior. Subsequently, a decrease in shear stress occurred with increasing shear rate (i.e., up sweep), which is shown in Figure 5. The apparent shear thickening is more pronounced for a preshear treatment at 25 s^{-1} compared to 5 s^{-1}. In addition, the stress curves did not exhibit such a maximum anymore when the shear rate was decreased (down sweep). Obviously, the initial structure could not be reformed within the time scale of the down sweep.[13]

In addition, hysteresis effects were observed for Ca−caseinate when comparing the shear stress curves obtained with increasing shear rates and decreasing shear rates. This implies that structural changes may have taken place due to the shear history. A resting

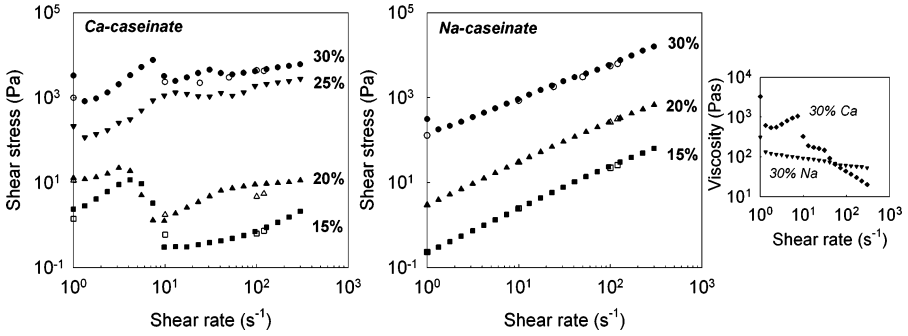

Figure 4. Shear stress as function of shear rate (up sweep) of Ca−caseinate (15%, 20%, 25%, and 30%) and Na−caseinate (15%, 20%, and 30%) measured at 50 °C. Each shear rate was applied for 10 s (closed symbols; squares, triangles up, triangles down, and circles for 15%, 20%, 25%, and 30% caseinate, respectively). Transient measurements (data points taken at shear rates that were applied for 60 s; open symbols) are included as well. The inset shows the viscosity as function of shear rate for 30% Ca−caseinate and 30% Na−caseinate.

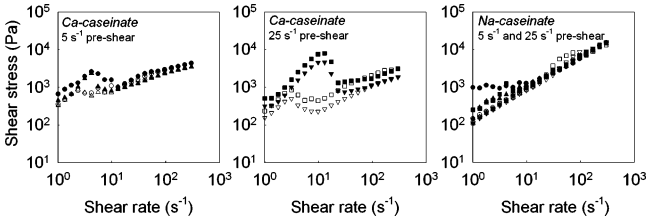

Figure 5. Shear stress as function of shear rate of 30% Ca−caseinate and 30% Na−caseinate measured at 50 °C after applying a preshear treatment at 5 s^{-1} (circles) and 25 s^{-1} (squares) for 2 min. The effect of a resting time of 7 min followed by again a preshear treatment at 5 s^{-1} (triangles up) and 25 s^{-1} (triangles down) for 2 min is also displayed. The flow curves for increasing (up sweep) and decreasing (down sweep) shear rates (each applied for 10 s) are denoted with closed and open symbols, respectively.

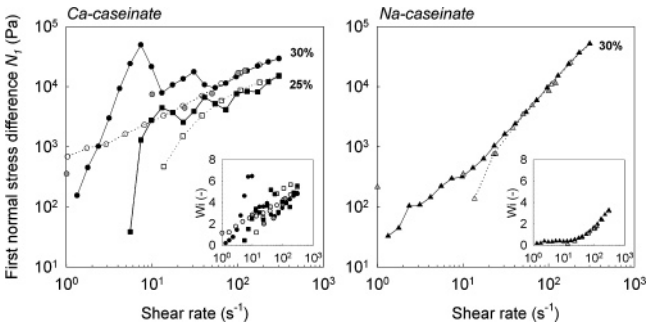

Figure 6. First normal stress difference N_1 as function of shear rate of 25% Ca−caseinate (squares), 30% Ca−caseinate (circles), and 30% Na−caseinate (triangles) measured at 50 °C. The curves for both increasing (up sweep) and decreasing (down sweep) shear rates are denoted with closed and open symbols, respectively. Data obtained from transient measurements at a constant shear rate are denoted with filled gray symbols. The insets depict the Weissenberg number as function of shear rate. (The same symbols are used as for N_1.)

time of 7 min resulted in the same shear stress curves, thus exhibiting shear thickening during the up sweep and hysteresis based on the down sweep, albeit both at slightly lower absolute shear stress values. This indicates that the caseins were able to return to their initial situation at least to a certain extent, and therewith showing a subtle time dependency. Dense Na−caseinate behaved in all cases slightly shear thinning, independent of either a preshear applied or resting time. These results suggest that 30% Na−caseinate exhibits an almost time-independent flow behavior, in contrast to 30% Ca−caseinate.

Finally, during the transient measurements at various shear rates, we observed a fluctuating behavior of the shear stress for 30% Ca−caseinate, implying instable flow behavior, whereas no such fluctuations were observed for 30% Na−caseinate.

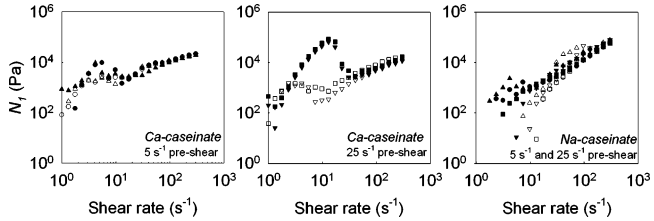

Figure 7. First normal stress difference N_1 as function of shear rate of 30% Ca−caseinate and 30% Na−caseinate measured at 50 °C after applying a preshear treatment at 5 s^{-1} (circles) and 25 s^{-1} (squares) for 2 min. The effect of a resting time of 7 min followed by again a preshear treatment at 5 s^{-1} (triangles up) and 25 s^{-1} (triangles down) for 2 min is also displayed. The flow curves for increasing (up sweep) and decreasing (down sweep) shear rates (each applied for 10 s) are denoted with closed and open symbols, respectively.

Analogous to the shear-induced structure formation in polymer and colloidal systems, it may be possible that the interactions present in the Ca−caseinate dispersions, which affect the non-monotonic behavior of the flow curve, are important for the structure formation that we observed. In that case, it is likely that the type of interactions but also the protein concentration have a large effect on structure formation. The presence of calcium ions in Ca−caseinate dispersions results in attractive interactions and in large aggregates that are susceptible to shear. A decrease in protein concentration is expected to negatively influence the occurrence of attractive interactions, which could explain why we did not observe anisotropic structure formation for a 20% Ca−caseinate dispersion in contrast to 25% and 20% Ca−caseinate. The lack of attractive interactions in dense Na−caseinate dispersions makes these dispersions less susceptible to shearing as the structural elements remain small in size, i.e., 10−50 nm. One might speculate however that affecting the protein interactions (e.g., by reducing the stability of the dispersion or the solvent quality) might result in shear-induced structure formation in these dispersions as well.

Effect of Steady Shear on First Normal Stress Difference. Normal forces varying between 10^{-2} and 10 N were found for 25% and 30% Ca−caseinate and for 30% Na−caseinate in the shear rate range of 1−300 s^{-1}, whereas 20% Na−caseinate exhibited normal forces only at shear rates larger than 50 s^{-1}. Figure 6 displays the first normal stress difference N_1 as function of the shear rate obtained from both shear rate sweeps and transient measurements for the 30% caseinates. Ca−caseinate showed slightly higher values compared to Na−caseinate. The measured N_1 for 30% Ca−caseinate, and to lesser extent for 25% Ca−caseinate, also displays non-monotonic behavior with increasing shear rate, similarly as we observed for the shear stress. With decreasing shear rates (down sweep), we observe

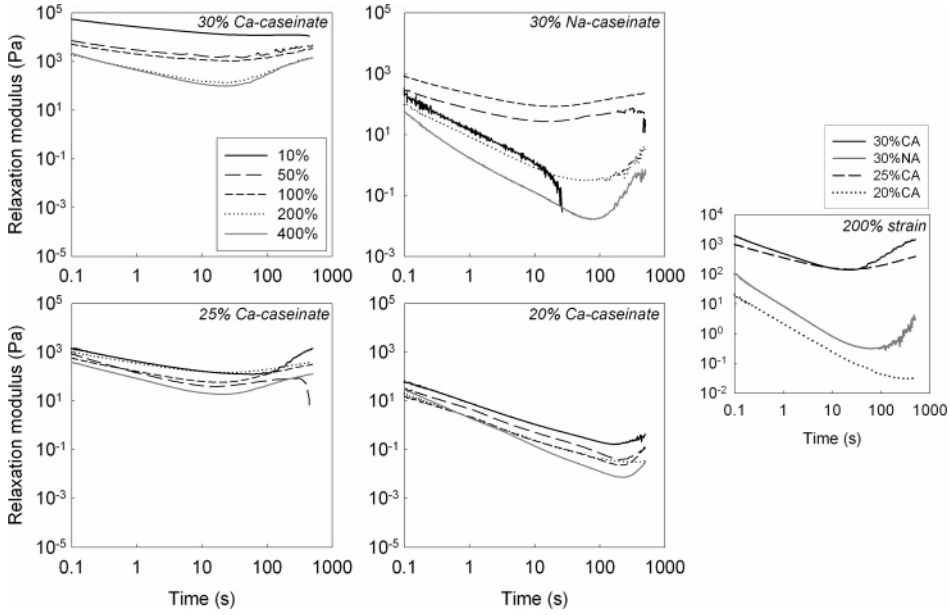

Figure 8. Strain-dependent relaxation modulus as function of time for 20%, 25%, and 30% Ca−caseinate and 30% Na−caseinate. Five nonlinear strain levels (i.e., 10%, 50%, 100%, 200%, and 400%) were applied at 50 °C.

a nearly perfect power law behavior of N_1. In contrast, N_1 for 30% Na−caseinate shows a power law behavior with both increasing and decreasing shear rate. The measured curves for the two caseinates show a crossover around 120 s^{-1}, after which $N_{1,Na} > N_{1,Ca}$. The transient N_1 values coincide best for 30% Na−caseinate as displayed in Figure 6. The resulting Weissenberg number ($Wi = N_1/\sigma$), often used to quantify the viscoelasticity of solutions, of 30% Ca−caseinate (and also for 25% Ca−caseinate) was higher compared to 30% Na−caseinate for the whole shear rate range, but the difference decreased to a factor 2 at the high shear rates (*Wi* of 4 and 2, respectively, for 120 s^{-1}), as depicted in Figure 6 (inset).

Figure 7 shows the effect of a preshear treatment of the evolution of N_1 as function of increasing and decreasing shear rate for both caseinates at a concentration of 30%. Again, N_1 of 30% Ca−caseinate shows non-monotonic behavior with increasing shear rate, whereas such behavior is not observed when the shear rate is decreased. The highest shear rate used for the preshear treatment resulted in the strongest increase in N_1. There is hardly an effect of resting time on N_1, confirming that the structures in the Ca−caseinate dispersion were able to quickly recover to their initial state. With the exception of the low shear rates (<10 s^{-1}), 30% Na−caseinate shows a power law relation of N_1 with the shear rate. The down sweeps deviate slightly from the up sweeps, and similarly to Ca−caseinate, no time-dependent effect on N_1 was observed for Na−caseinate.

We also observed fluctuations in normal stress during transient measurements of 30% Ca−caseinate, whereas 30% Na−caseinate did not show these strong irregular fluctuations (data not shown). Transient shear stress and normal stress were found to exhibit coupled oscillating behavior in micellar solutions in their nonlinear region,[9,27] which might indicate that a comparable mechanism caused these oscillations in Ca−caseinate.

Effect of Strain on Time Dependency of Relaxation Modulus. Figure 8 shows the behavior of the time-dependent and strain-dependent (at nonlinear strain values) relaxation modulus for various Ca−caseinate and Na−caseinate dispersions. The relaxation modulus for 25% and 30% Ca−caseinate decreases relatively slowly with time compared to 30% Na−caseinate and 20% Ca−caseinate. The latter two dispersions can be considered more liquidlike, whereas the former dispersions can be regarded as more solidlike. Obviously, the stronger interactions present in 25% and 30% Ca−caseinate dispersions result in a network-like structure. Qualitatively we can deduce that the relaxation times of 25% and 30% Ca−caseinate are of a larger time scale compared to those of 30% Na−caseinate and 20% Ca−caseinate. This may suggest that shear flow is more likely to influence the structure of the 25% and 30% Ca−caseinate dispersions rather than 30% Na−caseinate and 20% Ca−caseinate. In addition, the lack of a caseinate network prevents structures over long distances from being formed as observed for 20% Ca−caseinate. Another explanation could be that although the 20% Ca−caseinate dispersion is influenced by shear as shown in Figure 4 the mobility in the 20% dispersion could be too large for the enzymatic reaction to fix the structural change. All measured caseinate dispersions show a distinctive minimum in the measured relaxation modulus, which may be a feature of the dispersions. After the minimum, the relaxation modulus converges to an apparent steady-state value. Time-dependent changes during the measurements, such as drying at the edges of the dispersions, may also account for the observed increase in relaxation modulus after the minimum.

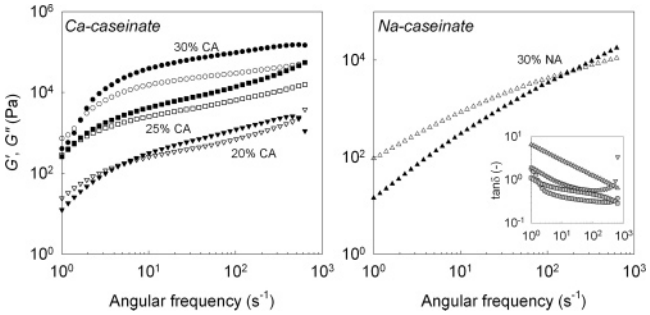

Figure 9. Mechanical spectra comprising G' (closed symbols), G'' (open symbols), and tan δ (inserted graph) as function of angular frequency ω of 20% Ca−caseinate (triangles down), 25% Ca−caseinate (squares), 30% Ca−caseinate (circles), and 30% Na−caseinate (triangles up) measured at 50 °C.

Linear Viscoelastic Properties. Figure 9 displays the frequency dependency of G' and G'' of 20%, 25%, and 30% Ca−caseinate and 30% Na−caseinate dispersions measured at 50

°C. All dense caseinates show crossovers of G'' and G' (tan $\delta = 1$), which fall in the lower frequency range for Ca−caseinate ($10^{\circ} < \omega < 10^{1}$ s^{-1}) and in the high-frequency range for Na−caseinate ($10^{2} < \omega < 10^{3}$ s^{-1}). The inverse of the angular frequency at which G'' and G' show a crossover, which is the longest relaxation time τ, provides an indication of the difference in interactions between Ca− and Na−caseinate.[32] From Figure 9, we can roughly estimate that for the 30% caseinates $\tau_{Ca} \approx 100\tau_{Na}$, which again confirms that much stronger physical interactions are present in 30% Ca−caseinate compared to those in 30% Na−caseinate, most likely caused by the calcium ions.[23] With decreasing Ca−caseinate concentration, the relaxation time decreases. When we compare the structure formation of the various caseinate dispersions, we find a transition in structure (from anisotropic to isotropic) when the Ca−caseinate concentration is decreased from 25% to 20%. This suggests that there is a critical region in terms of relaxation time for a caseinate dispersion to form anisotropic structures during shearing. Our results indicate that such a critical region for the relaxation time may exist in the range of $0.13 < \tau < 0.5$ s. Na−caseinate lies far from this critical region as its relaxation time is of a much shorter time scale.

To compare, the inverse of the so-called critical shear rate at which shear thinning starts to occur reflects a system-specific relaxation time τ_{rel}.[15, 33] Even though the measured flow curves in Figure 4 do not allow the determination of this shear rate, we may state that this critical shear rate is presumably a few orders of magnitude lower for 30% Ca−caseinate compared to the shear rate for 30% Na−caseinate when considering the measured flow curves; thus $\tau_{rel,\,Na} \ll \tau_{rel,\,Ca}$. This is in line with the results from the oscillatory measurements.

The relatively long relaxation times of the three Ca−caseinate dispersions reflect their solidlike behavior at 50 °C throughout the probed frequency range, which was also indicated by rather low tan δ values of ∼0.35. Na−caseinate is much more frequency-dependent compared to Ca−caseinate. The lowest tan δ value that was measured for Na−caseinate was ∼0.67. In addition, the fact that 30% Ca−caseinate tended to show a plateau in G' implies that this system is stronger "entangled" and less transient compared to Na−caseinate.[14]

Besides providing an indication of the interactions present in protein dispersions, the relaxation times as deduced from Figure 9 make it plausible that applying shear flow on Ca−caseinate and Na−caseinate has a different outcome in terms of structure formation and even for Ca−caseinate dispersions with different protein concentrations. Balancing physical caseinate properties, such as the relaxation time, and processing parameters, such as the shear rate, which is also indicated by the general Deborah number,[34] offers a means to screen caseinate dispersions for their potential to form shear-induced structures. However, for the caseinate systems investigated here, we conclude that shear-induced structure formation only occurs if the starting dispersion is susceptible to ordering, which means that structural elements need to be present.

Conclusions

A detailed investigation of the properties of dense Ca− and Na−caseinate dispersions has led to the insight that the initial physical and rheological properties of dense caseinate dispersions are of crucial importance for the structure formation encountered after shearing and enzymatic cross-linking of these industrially relevant dispersions.

Fiber formation due to shearing and enzymatic cross-linking is not a generic feature of caseinates yet, as we found isotropic materials for dense Na−caseinate and highly anisotropic materials for dense Ca−caseinate at similar processing conditions. This study reveals that changing the counterion affects the rheological behavior to a large extent, leading to completely different product structures. Larger micellar structural elements and pronounced attractive interactions in Ca−caseinate due to the presence of calcium compared to Na−caseinate explain its rheological behavior and account for the formation of anisotropic structures. This leads us to the conclusion that shear-induced structure formation only occurs if the starting dispersion is susceptible to ordering by shear.

For Ca−caseinate dispersions, the caseinate concentration is also of importance for shear-induced structure formation. A transition in structure formation occurs between 20% and 25% Ca−caseinate from isotropic to anisotropic structures, which may be related to a critical region of material-specific relaxation times that should be in balance with the shear rate applied. We think that besides the presence of structural elements the ability to form long-range anisotropic structures is also determined by the number of structural elements, which can result in a networklike structure at concentrated conditions.

Finally, the industrially relevant protein mixtures seem to show similarities with model materials often used to study shear-induced structure formation, such as the types of structures and the rheological behavior. The main similarities observed in the latter behavior were non-monotonic flow behavior, significant normal stresses, and the presence of attractive interactions.

Acknowledgment. This project is supported with a grant of the Dutch Programme EET (Economy, Ecology, Technology), a joint initiative of the Ministries of Economic Affairs, Education, Culture, and Sciences and of Housing, Spatial Planning, and the Environment. The program is managed by the EET Programme Office, SenterNovem. The authors thank A. van Aelst from the Wageningen Electron Microscopy Centre for preparing the SEM images, C. Klein and L. Sagis (Food Physics Group, Wageningen University) and P. Fischer (Food Process Engineering, ETH Zürich) for discussions on the rheological measurements, and M. Paques from Friesland Foods for fruitful discussions.

References and Notes

(1) Manski, J. M.; Van der Goot, A. J.; Boom, R. M. *Biomacromolecules* **2007**, *8*, 1271−1279.
(2) Belzung, B.; Lequeux, F.; Vermant, J.; Mewis, J. *J. Colloid Interface Sci.* **2000**, 224, 179−187.
(3) Wang, S. Q. *Macromolecules* **1991**, *24*, 3004−3009.
(4) Lyon, M. K.; Mead, D. W.; Elliott, R. E.; Leal, L. G. *J. Rheol.* **2001**, *45*, 881−890.
(5) Michele, J.; Patzold, R.; Donis, R. *Rheol. Acta* **1977**, *16*, 317−321.
(6) Scirocco, R.; Vermant, J.; Mewis, J. *J. Non-Newtonian Fluid Mech.* **2004**, *117*, 183−192.
(7) Won, D.; Kim, C. *J. Non-Newtonian Fluid Mech.* **2004**, *117*, 141−146.
(8) Vermant, J.; Raynaud, L.; Mewis, J.; Ernst, B.; Fuller, G. G. *J. Colloid Interface Sci.* **1999**, *211*, 221−229.
(9) Azzouzi, H.; Decruppe, J. P.; Lerouge, S.; Greffier, O. *Eur. Phys. J. E* **2005**, *17*, 507−514.
(10) Fischer, P.; Wheeler, E. K.; Fuller, G. G. *Rheol. Acta* **2002**, *41*, 35−44.
(11) Lopez-Gonzalez, M. R.; Holmes, W. M.; Callaghan, P. T. *Soft Matter* **2006**, *2*, 855−869.
(12) Schubert, B. A.; Wagner, N. J.; Kaler, E. W.; Raghavan, S. R. *Langmuir* **2004**, *20*, 3564−3573.
(13) Grand, C.; Arrault, J.; Cates, M. E. *J. Phys. II* **1997**, *7*, 1071−1086.
(14) Farrer, D.; Lips, A. *Int. Dairy J.* **1999**, *9*, 281−286.
(15) Panouille, M.; Benyahia, L.; Durand, D.; Nicolai, T. *J. Colloid Interface Sci.* **2005**, *287*, 468−475.
(16) Panouillé, M.; Durand, D.; Nicolai, T. *Biomacromolecules* **2005**, *6*, 3107−3111.

(17) Karlsson, A. O.; Ipsen, R.; Schrader, K.; Ardo, Y. *J. Dairy Sci.* **2005**, *88*, 3784−3797.
(18) Solanki, G.; Rizvi, S. S. H. *J. Dairy Sci.* **2001**, *84*, 2381−2391.
(19) Velez-Ruiz, J. F.; Barbosa-Canovas, G. V. *J. Texture Stud.* **2000**, *31*, 315−333.
(20) Lucey, J. A.; Srinivasan, M.; Singh, H.; Munro, P. A. *J. Agric. Food Chem.* **2000**, *48*, 1610−1616.
(21) De Kruif, C. G. *J. Dairy Sci.* **1998**, *81*, 3019−3028.
(22) Dickinson, E.; Semenova, M. G.; Belyakova, L. E.; Antipova, A. S.; Il'in, M. M.; Tsapkina, E. N.; Ritzoulis, C. *J. Colloid Interface Sci.* **2001**, *239*, 87−97.
(23) *Industrial Proteins in Perspective*, 1st ed.; Aalbersberg, W. Y., Hamer, R. J., Jasperse, P., de Jongh, H. H. J., De Kruif, C. G., Walstra, P., de Wolf, F. A., Eds.; Progress in Biotechnology 23; Elsevier Science: Amsterdam, 2003; p 284.
(24) Yokoyama, K.; Ohtsuka, T.; Kuraishi, C.; Ono, K.; Kita, Y.; Arakawa, T.; Ejima, D. *J. Food Sci.* **2003**, *68*, 48−51.
(25) Manski, J. M.; Van der Zalm, E. E. J.; Van der Goot, A. J.; Boom, R. *Food Hydrocolloids*, in press.
(26) Macosko, C. W. *Rheology: Principles, Measurements, and Applications*; Wiley-VCH: New York, 1994; p 550.
(27) Fischer, P. *Rheol. Acta* **2000**, *39*, 234−240.
(28) Radulescu, O.; Olmsted, P. D.; Decruppe, J. P.; Lerouge, S.; Berret, J. F.; Porte, G. *Europhys. Lett.* **2003**, *62*, 230−236.
(29) Vermant, J. *Curr. Opin. Colloid Interface Sci.* **2001**, *6*, 489−495.
(30) Acharya, D. P.; Sharma, S. C.; Rodriguez-Abreu, C.; Aramaki, K. *J. Phys. Chem. B* **2006**, *110*, 20224−20234.
(31) Stieger, M.; Richtering, W. *Macromolecules* **2003**, *36*, 8811−8818.
(32) Ponche, A.; Dupuis, D. *J. Non-Newtonian Fluid Mech.* **2005**, *127*, 123−129.
(33) Menjivar, J. A.; Rha, C. K. *Rheol. Acta* **1980**, *19*, 212−219.
(34) Forster, S.; Konrad, M.; Lindner, P. *Phys. Rev. Lett.* **2005**, *94*, 17803.

BM700885F